Int J Adv Manuf Technol (2017) 90:309–316
DOI 10.1007/s00170-016-9329-2

ORIGINAL ARTICLE

Electromagnetic attractive forming of sheet metals by means of a dual-frequency discharge current: design and implementation

Quanliang Cao [1,2] · Zhipeng Lai [1,2] · Qi Xiong [1,2] · Qi Chen [1,2] · Tonghai Ding [1,2] · Xiaotao Han [1,2] · Liang Li [1,2]

Received: 13 May 2016 / Accepted: 15 August 2016 / Published online: 31 August 2016

Abstract The ability to generate an attractive force for electromagnetic forming is an interesting and challenging issue, compared with conventional electromagnetic repulsion processes. This work presents a discharge system with two sets of power supplies and a timing control system for the production of a dual-frequency discharge current in a single coil. The discharge current can be employed to generate an attractive force between the coil and the workpiece in the forming process. The effectiveness of the system was verified both by numerical simulations and by a series of experiments of sheet metal forming. Our results show that an AA 1060 aluminum alloy sheet with a thickness of 1 mm, at a distance of 9 mm from the coil bottom, can be attracted towards the coil with a maximum deformation of about 4.7 mm. We also demonstrate that there is an optimum value for deformation depth, which is related to the initial discharge voltage of the fast discharge system. The presented method and results can be helpful in designing electromagnetic forming systems and widening their applications.

Keywords Electromagnetic forming · Electromagnetic attractive force · Pulsed magnetic field · Discharge current

✉ Xiaotao Han
xthan@mail.hust.edu.cn

[1] Wuhan National High Magnetic Field Center, Huazhong University of Science and Technology, Wuhan 430074, People's Republic of China

[2] State Key Laboratory of Advanced Electromagnetic Engineering and Technology, Huazhong University of Science and Technology, Wuhan 430074, People's Republic of China

1 Introduction

Electromagnetic forming (EMF) is a high-speed and non-contact forming technology, which employs a pulsed electromagnetic force to reshape metallic workpieces with several advantages in comparison to the conventional forming processes, including improved formability and high integrity of the workpiece surface [1]. Research on this topic has been active since the 1960s, with a number of studies related to tube expansion or compression as well as sheet metal forming. However, most research efforts focus on the development of EMF with repulsive forces between the EMF coil and the conductive workpiece [2–5].

In addition to conventional repulsive forces, the EMF process can be realized by use of attractive forces, which can widen its application range to other processes such as external dent repair and disassembly of press-fit joints. Nevertheless, the generation of efficient attractive magnetic forces between the coil and the workpiece is a challenging task, which results in relatively little information on the attractive process that has been published so far. To the best of our knowledge, there are currently three main types of methods to achieve an attraction EMF process: (1) use of discharging current with a low frequency to generate an attractive force between the coil and a ferromagnetic sheet. This method is only effective for workpieces made of magnetic materials, since high-gradient magnetic forces are needed to compete with conventional Lorentz forces [6]; (2) use of an additional attracting screen made of conductive materials to generate an attractive force between the screen and the workpiece [7]. The basic principle of this method is that the induced currents flowing in the screen and in the sheet have the same direction. A main drawback of the method is that the EMF system must have enough space to accommodate the coil, and thus, the distance between the screen and the workpiece can reach prohibitively large values in the applications, resulting in a poor

efficiency; and (3) sequential use of slow and fast frequencies of discharge current to generate an attractive force between the coil and the conductive workpiece. This method has been attracting significant attention, resulting in several patents, which were recently reviewed by Batygin et al. [6]. Among these patents, Zieve proposed a power supply system for the generation of a continuous discharge current in the coil containing both slow and fast frequencies without interrupting the discharge forcibly [8]. Based on the continuous discharge current, the attractive EMF process can be realized by just one coil, and the configuration of coil and workpiece is much similar to that in conventional repulsive EMF processes. Therefore, this EMF system could be more practical, compared with other attractive forming processes. The ability of a similar current for generating attractive force between coil and workpiece was numerically confirmed by Deng et al. [9]. However, relatively little published information is available for the practical design and the implementation of such a special current at present, and the deformation behavior of the workpiece under the action of this type of current should be further investigated.

The objective of this work is mainly to discuss the design and implementation of an electromagnetic forming system based on an attractive process. Starting with the analysis of the electromagnetic forces acting on the sheet metal, the basic principle and design of an electromagnetic system for producing an attractive force in the forming process are presented. Both numerical simulations and experimental results on the forming of an AA1060 sheet are presented to support our design.

2 Principle and design

For the purpose of the following analysis, the schematic drawing of the electromagnetic sheet forming system used in this work is presented in Fig. 1, where the coil is coaxial and concentric with the sheet and only half view of the system could be modeled in the simulation due to the axial symmetry. The following numerical analysis is solved by use of the COMSOL Multiphysics package (V4.3b), and more details on the simulation method can be found in our previous work [10].

2.1 Basic principle of electromagnetic forming with attractive force

When a time-varying current flows through into a coil in an EMF system, a pulsed magnetic field is generated, and an eddy current will be induced in the workpiece. As a result, a strong repulsive electromagnetic force for the rapid deformation of the workpiece could be created, and its density $\overrightarrow{f_m}$ can be expressed as:

$$\overrightarrow{f_m} = \overrightarrow{J_e} \times \overrightarrow{B}, \tag{1}$$

where $\overrightarrow{J_e}$ and $\overrightarrow{B}$ respectively indicate the eddy current density and magnetic flux density in the workpiece. In the axisymmetric case, the eddy current density $\overrightarrow{J_e}$ only has a circumferential component $\overrightarrow{J_{\mathrm{ephi}}}$, and thus, $\overrightarrow{f_m}$ can be further decomposed into a radial component f_{mr} and an axial component f_{mz}, which can be written according to the following equations:

$$f_{\mathrm{mr}} = J_{\mathrm{ephi}} \times B_z \tag{2}$$

$$f_{\mathrm{mz}} = -J_{\mathrm{ephi}} \times B_r, \tag{3}$$

where B_r and B_z are the two components of $\overrightarrow{B}$. The axial component of the electromagnetic force in Eq. (3) is the main cause of deformation in Fig. 1, and the negative value predominates in the deformation process which tends to push the workpiece away from the coil independent of the initial current direction. We point out that it is a challenging issue to alternate the force direction by changing the relative directions of the eddy current and radial magnetic field based on Eq. (3), due to the coupling between

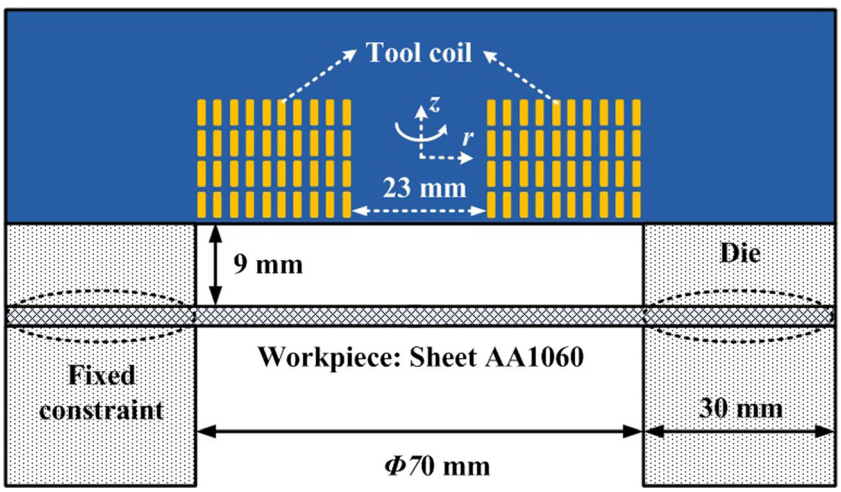

Fig. 1 Schematic geometry of the electromagnetic sheet metal forming system

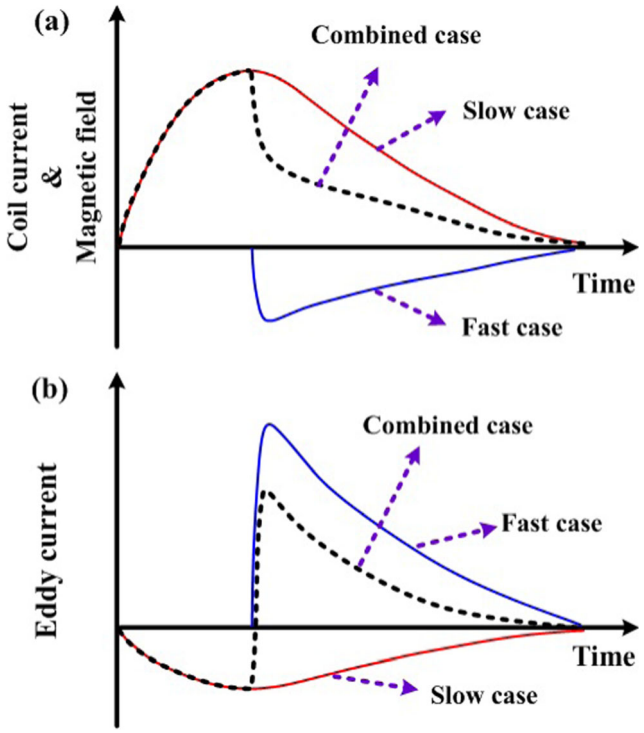

Fig. 2 Schematic diagram of the design principle of discharge current for producing attractive forces. **a** Expected coil current and magnetic field; **b** expected eddy current in the workpiece

the two variables in conventional EMF systems. A possible solution to this problem, through decoupling control of the magnetic field and eddy current in the workpiece, is proposed in this work with the aid of a dual-frequency discharge current in Fig. 2a. When the slow and fast discharges work together, f_{mz} in Eq. (3) can be replaced by

$$f_{mz} = -\left(J_{ephi\_slow} + J_{ephi\_fast}\right) \times \left(B_{r\_slow} + B_{r\_fast}\right), \quad (4)$$

where J_{ephi_slow} and J_{ephi_fast} denote the densities of eddy currents induced by the time-varying currents in the slow and fast discharge system, and B_{r_slow} and B_{r_fast} indicate the flux densities of the radial magnetic fields generated by the two discharge systems, respectively. In order to change the direction of the electromagnetic force acting on the workpiece, the directions of the slow and fast discharge currents should be opposite, and the following requirements related to the characteristics of the dual-frequency discharge current need to be satisfied.

(1) As shown in Fig. 2a, the amplitude of the fast discharge current I_{coil_fast} (fast case) should be smaller than that of the slow discharge current I_{coil_slow} (slow case) in order to leave the direction of generated magnetic field unchanged.
(2) As shown in Fig. 2b, conversely, the density of the eddy current J_{ephi_fast} induced by the fast discharge current (fast case) should be larger than that induced by the slow discharge current J_{ephi_slow} (slow case) to change the direction of the eddy current in the workpiece. Since the induced eddy current is proportional to the change rate of discharge current according to Faraday's law, this requirement can be met even though I_{coil_slow} is larger than I_{coil_fast} through decreasing the rising edge time of the discharge current I_{coil_fast} for greatly increasing its change rate.
(3) The fast discharge current should be introduced close to the peak time of magnetic field generated by the slow discharge current in order to obtain a relatively large electromagnetic force.

2.2 Design and implementation

In the previous section, we demonstrated that it is possible to generate an attractive force for sheet deformation by using the discharge current in Fig. 2. However, such a current cannot be

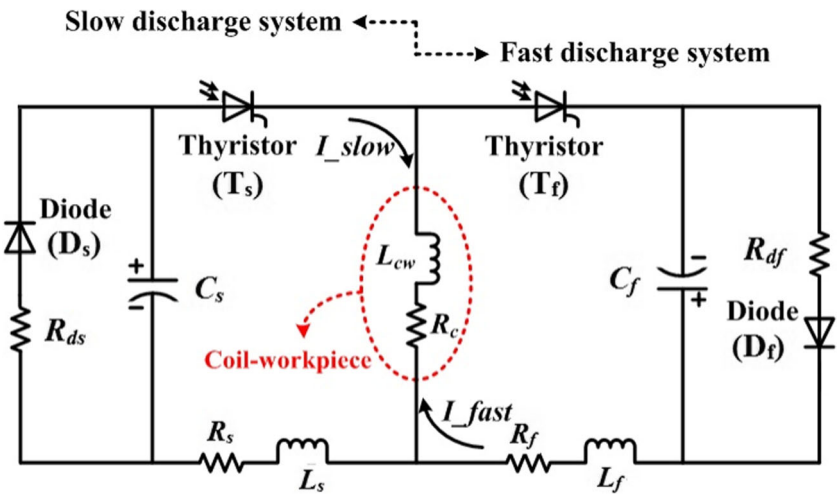

Fig. 3 Schematic diagram of the electrical circuit of the EMF system for attractive forming process. The *dotted box* depicts the equivalent circuit of the coil-workpiece system

Table 1 Circuit parameters for designed EMF system in Fig. 1

Symbol	Description	Value
Slow discharge system		
C_s	Capacitance	2880 μF
U_{s0}	Initial discharge voltage	8 kV
R_s	Line resistance	≈0.35 Ω
L_s	Line inductance	≈1.7 mH
R_{ds}	Crowbar resistance	≈0.2 Ω
Fast discharge system		
C_f	Capacitance	160 μF
U_{f0}	Initial discharge voltage	0 ~ 6 kV
R_f	Line resistance	≈8 mΩ
L_f	Line inductance	≈10 μH
R_{df}	Crowbar resistance	≈10 mΩ
Coil_workpiece		
Rc	Resistance	≈25 mΩ
Lcw	Equivalent inductance	≈45 μH

achieved through the conventional discharge circuit configuration used in the EMF system. In fact, the dual-frequency discharge current, which consists of a slow-rise and a rapid-decline stage, can be seen as a combination of two different currents. This means that the desired current can be obtained by using two sets of discharge systems. On this basis, a new discharge circuit configuration is proposed, and its detailed information is described as follows:

(1) Two sets of discharge systems with different electrical parameters including capacitances and inductances for generating slowly and fastly varying currents, as shown in the left and right parts of Fig. 3, corresponding to the slow and fast discharge systems. The line inductance and resistance in the slow discharge system are much larger than that in the fast discharge system.

(2) Each discharge system has an additional crowbar circuit consisting of a diode and a resistor, which is connected in parallel to the capacitor to regulate the current waveform flowing in the coil.

(3) The two capacitor banks in the discharge systems are electrically connected to a single tool coil with opposite electrical charges.

(4) Light-activated thyristors are used as controllable switches to trigger the time of the two discharge systems with the aid of a timing control system.

Compared with the power supply system reported by Zieve [8], the most remarkable advantage of the proposed discharge system is that the power supply circuit is much simpler and easier to implement. The detailed electrical parameters are listed in Table 1. In the EMF process, the light-activated thyristor T_s is first triggered at the beginning of the process, and the slow discharge system works until the end, while the fast discharge system only starts to work when the current in the coil reaches a maximum through triggering the light-activated thyristor T_f at that time. The current waveforms with the circuit configuration in the case of U_{s0} = 8000 V and U_{f0} = 3200 V are shown in Fig. 4, according to the MATLAB/simulink results obtained assuming that the electrical parameters of the coil-workpiece system are kept constant in the forming process. When there is no fast discharge system, the coil current I_{coil_1} is equal to the current of I_{slow_1} flowing

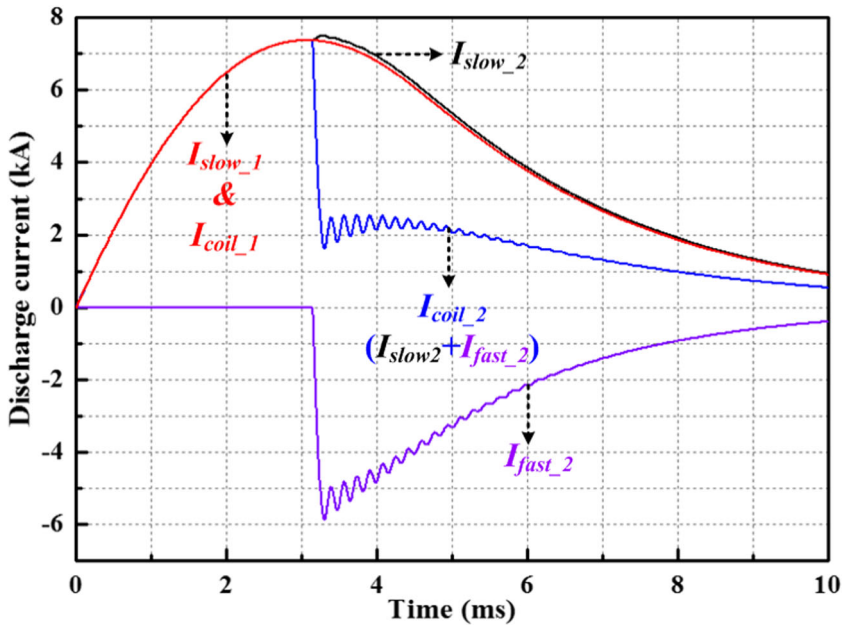

Fig. 4 Waveforms of discharge currents in different branches. *Subscript* "*1*" denotes the case in the absence of fast discharge system, and "*2*" indicates the case in the presence of fast discharge system

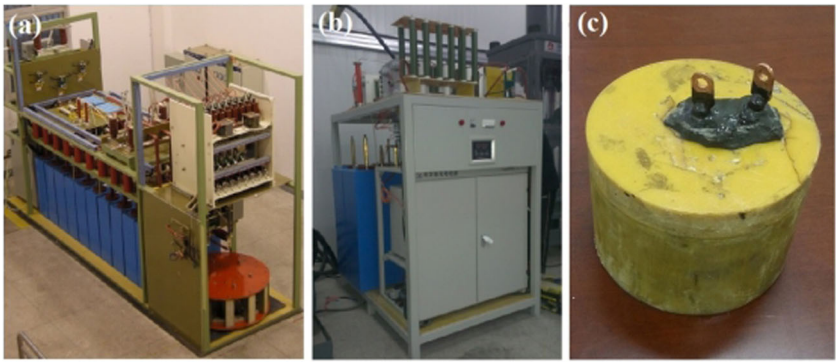

Fig. 5 Photos of the main setup components used in the experiment. **a** Power supply for slow discharge system with parameters of 1 MJ/25 kV/3.2 mF; **b** power supply for fast discharge system with electrical parameters of 1 MJ/25 kV/3.2 mF; **c** forming coil

in the slow discharge system with a relatively long rise time of about 3.1 ms. When the fast discharge system is triggered at the time of 3.15 ms in line with the experimental conditions, the subsequent attenuation of coil current I_{coil_2} is much faster compared to the case without the fast discharge system, which is due to the fact that a negative current I_{fast_2} with a short rise time of 0.15 ms is generated by the fast discharge system for lowering the coil current. Furthermore, it can be seen that the fast discharge system has little effect on the current flowing in the slow discharge system according to the curves of I_{slow_1} and I_{slow_2}. This point is in accordance with the design since the majority of the current generated by the fast discharge system is expected to flow in the coil-workpiece system.

To generate the required discharge current flowing in a single coil, two existing capacitor-type pulse power supplies in the authors' laboratory have been used for the experiments. The 1-MJ capacitor bank shown in Fig. 5a with a total capacitance of 3.2 mF and maximum discharge voltage of 25 kV was used for the slow discharge system, and the 200-kJ capacitor bank shown in Fig. 5b with a total capacitance of 640 μF and maximum discharge voltage of 25 kV was selected for the fast discharge system. It should be noted that both the capacitance and the initial discharge voltage of the two capacitor banks are adjustable according to the experimental requirements, and the selected values of these parameters in the experiments are listed in Table 1. A coil constituted by 40 total turns, as depicted in Fig. 1, was fabricated by copper conductors with rectangular cross-section of 1×4 mm^2 and was reinforced by Zylon fibers, which have an inner diameter of 23 mm, an outer diameter of 70 mm, and a height of 17.5 mm for the space filling with copper conductors. The spaces between conductors along the r-axis and the z-axis in Fig. 1 are 1.5 and 0.5 mm, respectively. The coil was assembled together with epoxy resin as a forming coil unit, as shown in Fig. 5c.

3 Results and discussion

To validate the effectiveness of the proposed system for attractive forming, the investigation of deformation behavior of an AA1060 sheet was carried out both by simulation and experimental studies, whose results are presented in the following sections.

3.1 Simulated results

The physical parameters of AA1060-H28 including density (2.71 g/cm^3), electrical conductivity (62 % IACS), Young's modulus (69 GPa), and initial yield tensile strength (98 MPa) were used in the simulations, which were obtained from a database of engineering material properties (www.makeitfrom.com/material-properties/1060-H28-Aluminum/). The testing stress-strain curve ($\sigma_t - \varepsilon_t$) in Fig. 6 was derived from the engineering stress-strain curve ($\sigma_e - \varepsilon_e$) based on the following equations: $\sigma_t = \sigma_e(1 + \varepsilon_e)$ and $\varepsilon_t = \ln(1 + \varepsilon_e)$. The data of ($\sigma_e - \varepsilon_e$) were directly obtained from the quasi-static test. It should be noted that the above two equations are valid only for the homogeneous deformation. Therefore, an additional stress-

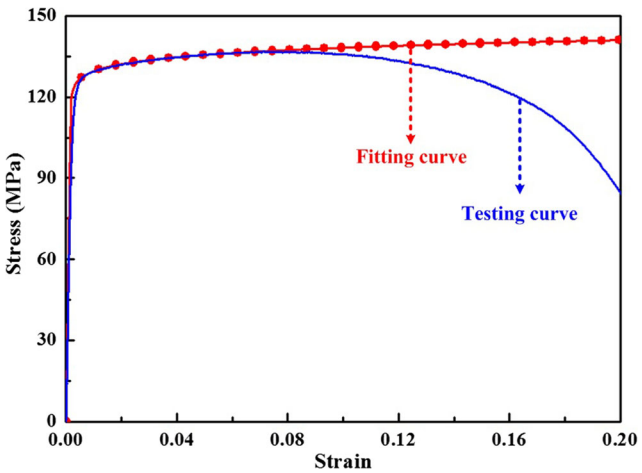

Fig. 6 Testing and fitting quasi-static stress-strain curves of the sheet material (AA1060) used in the experiments

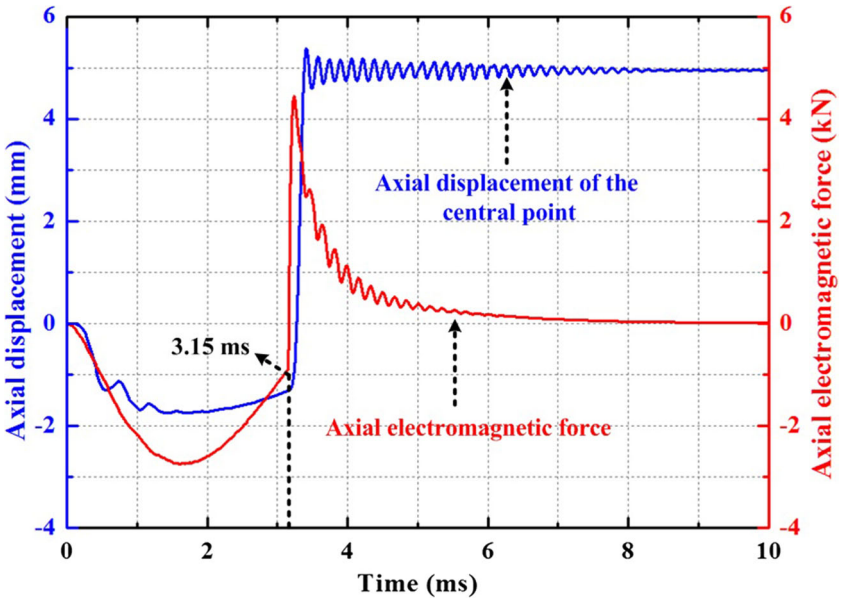

Fig. 7 Calculated axial displacement of sheet center and axial electromagnetic force acting on the sheet in the forming process in the case of U_{s0} = 8000 V and U_{f0} = 3200 V

strain curve in Fig. 6 was fitted using the stress-strain data of the testing curve before inhomogeneous deformation, which was taken to approximately reflect the true stress-strain of materials in the simulations. The expression of the fitting stress-strain curve can be given by

$$\sigma_{qs} = \begin{cases} E\varepsilon & \sigma_{qs} < \sigma_{qs0} \\ \sigma_{qs0} + A\varepsilon_p{}^B & \sigma_{qs} \geq \sigma_{qs0} \end{cases}, \quad (5)$$

where E represents Young's modulus, σ_{qs0} is the initial yield stress, ε_p is the plastic strain which can be expressed as $\varepsilon - \frac{\sigma_{qs}}{E}$, and A and B are two constants whose value is 50.87 and 0.0983 MPa, respectively. To consider the effect of plastic strain rate on the deformation behavior in the EMF process, the Cowper-Symonds constitutive model is adopted to approximately reflect the high-strain-rate effect [11]

$$\sigma = \sigma_{qs}\left[1 + \left(\frac{\varepsilon_p}{P}\right)^m\right], \quad (6)$$

where σ_{qs} is the quai-static stress in Eq. (5), ε_p is the plastic strain rate, P and m are 6500 s^{-1} and 0.25 for aluminum, respectively.

Figure 7 shows the calculated axial displacement at the sheet center and the axial electromagnetic force acting on the sheet in the forming process by using the given coil current I_{coil_2} in Fig. 4. It can be seen that the final displacement at the

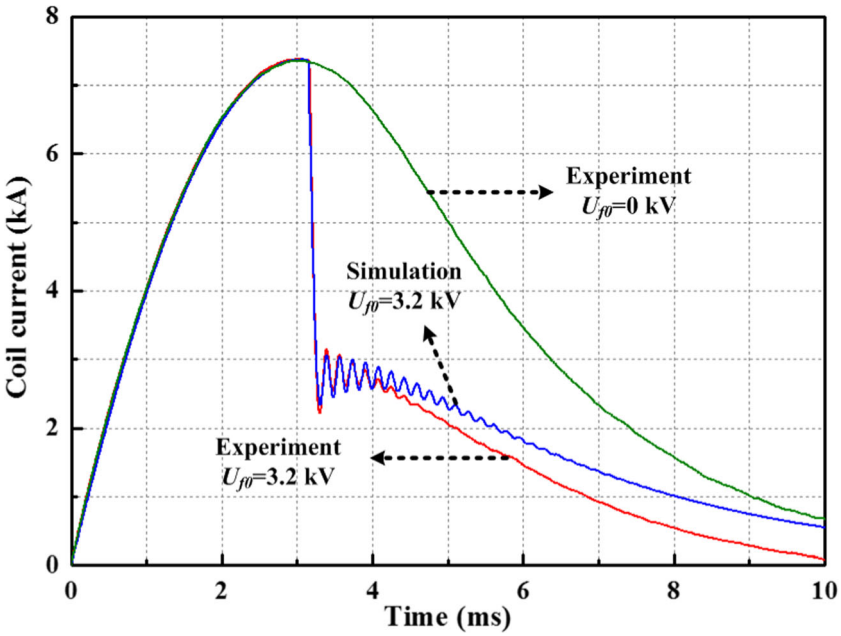

Fig. 8 Experimentally measured discharge currents in the two cases for different initial voltages of the fast discharge system (U_{f0})

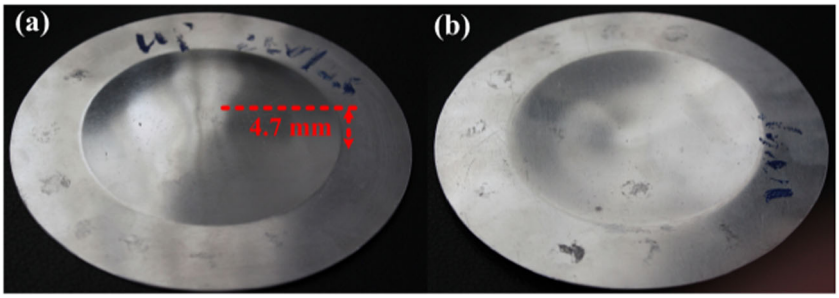

Fig. 9 Photos of the deformed sheet with front and back faces. **a** The face towards the coil; **b** the reverse side

center is ≈4.94 mm along the positive z-axis direction, which means the sheet has been deformed and attracted towards the coil. This point can be explained qualitatively according to the characteristics of the pulsed electromagnetic force in Fig. 7. It can be seen that a much larger attractive force with a positive value can be produced in the rapid-decline stage when the fast discharge system is applied at the time of 3.15 ms, compared with the lower repulsive force in the low-rise stage. Meanwhile, considering the influence of the current frequency on the deformation behavior, the pulsed magnetic field with a long rise time of about 3.15 ms in the low-rise stage produces a thicker skin depth which leads to significant magnetic field permeation through the 1-mm-thick sheet, resulting in a remarkable loss of the magnetic energy, eventually enabling the deformation under the action of attractive forces in the rapid-decline stage.

3.2 Experimental results

The workpiece used in this study was an AA 1060 sheet with a thickness of 1 mm. A nonmetal material of glass-fiber reinforced nylon was chosen for the die in order to avoid unnecessary eddy currents. In the experiments, the coil was first energized only by the slow discharge system with a 2880-μF capacitor, and the fast discharge stage was applied around the peak time of the slow discharge current (3.15 ms) via a 160-μF capacitor. The initial discharge voltages of the two systems are given in Table 1, in which the initial voltage of the fast discharge system U_{f0} varies within a certain range (0 ~ 6 kV) in order to analyze its impact on the sheet deformation. Figure 8 presents the measured discharge currents flowing through the coil in the two cases, i.e., U_{f0} = 3200 V and U_{f0} = 0 V. The calculated result in the case U_{f0} = 3200 V is also displayed for comparison. It can be seen that the measured current curves are consistent with the design prediction and show reasonable agreement with the simulation result. The shapes of the deformed sheet with both front and back faces are shown in Fig. 9, in which the sheet metal was deformed towards the coil surface with a maximum displacement of 4.7 mm at the central point. Furthermore, a series of experiments were carried out with different initial capacitor voltages of the fast discharge system, and the maximum displacements of the deformed sheets are shown in Fig. 10. It can be seen that there is an optimum voltage for the largest deformation around the value of U_{f0} = 3200 V and the experimental trend is almost the same as that obtained in the simulation. The main reason for this phenomenon is that the total magnetic flux density in Eq. (4) decreases with increasing U_{f0}; however, the total eddy current in the sheet increases with U_{f0}. These competing trends can yield an optimum value of U_{f0} for the generation of attractive electromagnetic forces in the deformation process.

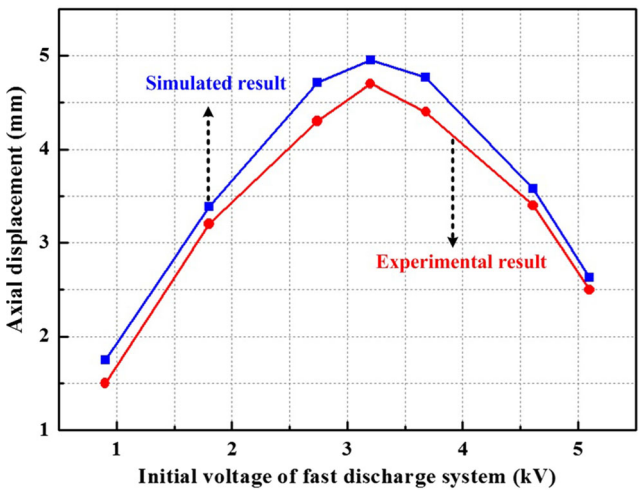

Fig. 10 Axial displacements of sheet center under different initial voltages of the fast discharge system

4 Conclusion

To generate a sufficiently intense pulsed electromagnetic force for attractive forming process with a single coil, an EMF system with two sets of power supply was designed, implemented, and tested. Both numerical and experimental results demonstrate that the designed EMF system can be applied to the attractive forming of a 1-mm-thick AA1060 sheet. Future work will focus on the optimization of the EMF system in order to achieve higher forming efficiency and ability through systematical and theoretical analysis as well as verification tests.

Acknowledgments This work was supported by the National Basic Research Program of China (973 Program): 2011CB012800 (2011CB012801) and the Program for New Century Excellent Talents in University (NCET-13-0225).

References

1. Psyk V, Risch D, Kinsey BL, Tekkaya AE, Kleiner M (2011) Electromagnetic forming—a review. J Mater Process Technol 211:787–829
2. Xu JR, Yu HP, Li CF (2013) Effects of process parameters on electromagnetic forming of AZ31 magnesium alloy sheets at room temperature. Int J Adv Manuf Technol 66:1591–1602
3. Noh HG, Song WJ, Kang BS, Kim J (2015) Two-step electromagnetic forming process using spiral forming coils to deform sheet metal in a middle-block die. Int J Adv Manuf Technol 76(9): 1691–1703
4. Kim JH, Kim D, Lee MG (2015) Experimental and numerical analysis of a rectangular helical coil actuator for electromagnetic bulging. Int J Adv Manuf Technol 78(5):825–839
5. Fan Z, Yu H, Meng F, Li C (2016) Experimental investigation on fabrication of Al/Fe bi-metal tubes by the magnetic pulse cladding process. Int J Adv Manuf Technol 83(5–8):1409–1418
6. Batygin YV, Golovashchenko SF, Gnatov AV (2013) Pulsed electromagnetic attraction of sheet metals—fundamentals and perspective applications. J Mater Process Technol 213(3):444–452
7. Batygin YV, Golovashchenko SF, Gnatov AV (2014) Pulsed electromagnetic attraction of nonmagnetic sheet metals. J Mater Process Technol 214(2):390–401
8. Zieve PB (1991) Power supply for electromagnetic proof load tester and dent remover. US Patent 5:046,345
9. Deng JH, Li CF, Zhao ZH, Tu F, Yu HP (2007) Numerical simulation of magnetic flux and force in electromagnetic forming with attractive force. J Mater Process Technol 184(1–3):190–194
10. Cao QL, Li L, Lai ZP, Zhou ZY, Xiong Q, Zhang X, Han XT (2014) Dynamic analysis of electromagnetic sheet metal forming process using finite element method. Int J Adv Manuf Technol 74(1–4): 361–368
11. Mamalis AG, Manolakos DE, Kladas AG, Koumoutsos AK (2006) Electromagnetic forming tools and processing conditions: numerical simulation. Mater Manuf Process 21(4):411–423